

## Design and Control of Inpipe Inspection Robot

<sup>1</sup>Ngo Cao Cuong , <sup>2</sup>Nguyen Thanh Phuong , <sup>3</sup>Duong Vu Van  
Hutech High Technology Institute

---

**ABSTRACT :** This paper proposes an inpipe inspection robot with the wall-pressing force adjustment using DC motor. It is developed for long distance inspection in sea-water pipelines such as horizontal pipelines and slope pipelines with large variable diameters from 600mm to 800mm. Its mechanical design consists of two modules as driving module and control module. The driving module has three pantograph type links spaced in 120° with three caterpillar track wheels. This design makes it possible to realize the adaptation to pipe diameter and the adjustment of wall-pressing force. The control module consists of a micro controller, motor driver and sensor interface. To control the inpipe inspection robot, firstly, the inpipe inspection robot is considered as a dynamic model of mass-spring-damper system. Secondly, an observer is designed to estimate the unknown wall-pressing force to sustain the robot in pipeline. Thirdly, an algorithm of wall-pressing force generator is presented to find out an appropriate reference value of wall-pressing force. Fourthly, PID fuzzy controller is designed to make the estimated wall-pressing force track the reference values irrelatively to variable diameter of pipeline. Finally, the driving tests results of the developed inpipe inspection robot are shown to prove the effectiveness of the proposed controller and the applicability of the developed inpipe inspection robot.

---

### I. INTRODUCTION

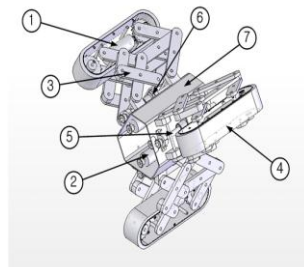
The domestic and foreign pipe equipments have been installed from the late 70's. So their safety is doubted by corrosion and defect due to their deterioration. Recently, to overcome these problems, several types of inpipe inspection robots such as PIG type, wheel type, wall-press type and caterpillar type are being introduced [4-5]. Wall-press type inpipe inspection robots of them have high performance to inspect vertical pipelines and curved pipelines. However, because most of the wall-press type robots use spring tension to press the inside wall of pipelines, these robots have many restrictions to control the wall-pressing force [1-2]. To solve this problem, a new inspection robot for pipelines with large variable diameters is needed. In this paper, a new wall-press type inpipe inspection robot, which is hybridized with caterpillar type and wall-press type, is proposed. To develop the inpipe inspection robot, firstly, an inpipe inspection robot is designed by 3D machine design program, and a prototype of the robot is presented. Secondly, dynamic model of the system is obtained by process model identification method. Thirdly, an observer is designed to estimate the unknown wall-pressing force to sustain the inpipe inspection robot in pipeline. Fourthly, PID fuzzy controller is designed to make the estimated wall-pressing force track the reference wall-pressing force irrelatively to variable diameter of pipeline with experimental results. Finally, the driving tests of the inpipe inspection robot are performed in horizontal pipelines and slope pipelines of 30°. The test results are shown to prove the effectiveness of the developed inpipe inspection robot in the practical industrial field.

### II. DESIGN OF AN INPIPE INSPECTION ROBOT

The active inspection robot consists of driving module and control module.

#### 2.1 Driving module

The driving module of the inpipe inspection robot is designed by 3D machine design program, Solid Works. The 3D designed robot is depicted in Fig. 1.



|                        |                 |
|------------------------|-----------------|
| ① Track wheel DC motor | ② Link DC motor |
| ③ Pantograph type link | ④ Track wheel   |
| ⑤ Ball screw           | ⑥ Slider        |
| ⑦ Body                 |                 |

Fig. 1 3D designed inpipe inspection robot.

The driving module has three pantograph type links spaced in 120° with three caterpillar track wheels. This design makes it possible to realize the adaptation to pipe diameter and the adjustment of wall-pressing force. A prototype of the active inspection robot is depicted in Fig. 2 based on 3D design. Table 1 shows the specification of the developed inpipe inspection robot.

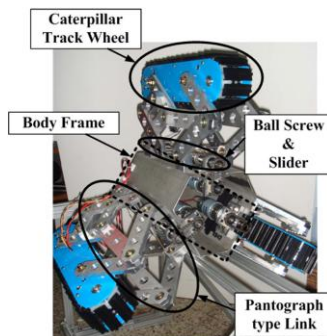


Fig. 2 Prototype of the inpipe inspection robot.

Table 1 Specification of the inpipe inspection robot.

| Item               | Value         |
|--------------------|---------------|
| Length of Robot    | 0.45m         |
| Weight of Robot    | 30kg          |
| Variable dimension | 0.53m ~ 0.88m |

## 2.2 Control module

The control module consists of a micro controller, motor driver and sensor interface. Fig. 3 shows about scheme of control system.

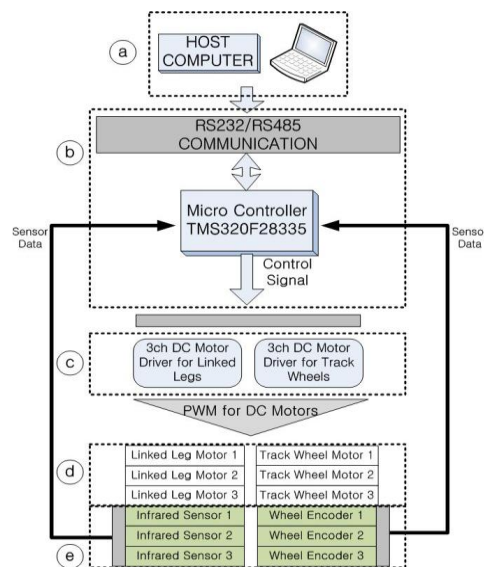


Fig. 3 Scheme of control system.

As shown in Fig. 3, (a), (b), (c), (d) and (e) are host computer, micro controller, DC motor driver, actuator and sensor part, respectively. A control system is developed based on DSP TMS320F28335. DC motor driver is controlled by PWM and the sensor interface consists of encoders and infrared sensors.

### III. MODELING OF THE INPIPE INSPECT-ION ROBOT

#### 3.1 Dynamic modeling

Fig. 4 shows the model of pantograph type link in the dashed line.

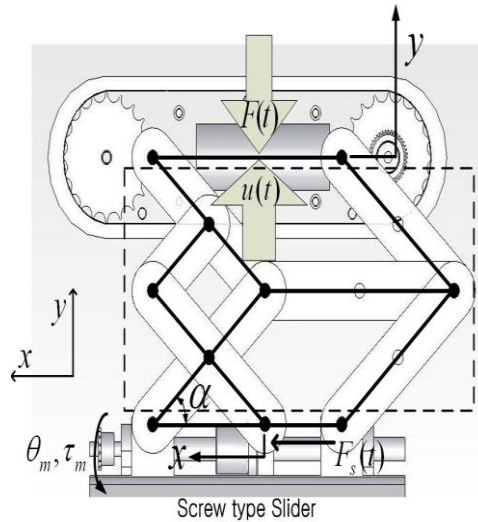


Fig. 4 Model of pantograph type link.

The screw type slider is rotated by torque of motor  $\tau_m$ . The slider is moved with slider force  $F_s(t)$  to x-axis.  $F_s(t)$  is transformed to y-axis direction force.  $u(t)$  is a force generated by pantograph type link, and  $y$  is a displacement of pantograph type link in the  $y$  direction.  $F(t)$  is the wall-pressing force. To simplify the model of pantograph type link, the pantograph type link is considered as mass-spring-damper model in Fig. 5. The parameters used for dynamic modeling are listed in Table 2.

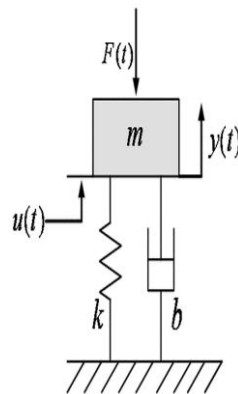


Fig. 5 Model of mass-spring-damper.

Table 2 Parameters of dynamic modeling.

| Parameter | Description                             |
|-----------|---|
| $u(t)$    | Model input                             |
| $F(t)$    | Wall pressing force                     |
| $F_s(t)$  | Transfer force of slider                |
| $x(t)$    | Displacement of slider                  |
| $y(t)$    | Displacement of pantograph type link    |
| $i_m$     | Armature current of motor               |
| $\tau_m$  | Rotational torque of motor              |
| $\sigma$  | Distance of screw pitch to pitch        |
| $T$       | Torque constant of motor                |
| $m$       | Mass of mass-spring-damper model        |
| $k$       | Spring constant of pantograph type link |
| $b$       | Damper constant of pantograph type link |

The dynamic model equation is as follow Eq. (1).

$$m\ddot{y} + b\dot{y} + ky = u - F \quad (1)$$

In this model,  $u(t)$  is model input and  $y$  is model output. The model input  $u$  is defined as Eq. (2).

$$u = A \frac{2\pi}{\sigma} \tau_m = A \frac{2\pi}{\sigma} T i_m \quad (2)$$

In Eq. (2),  $A$  is the linearization coefficient of relation  $x(t)$  to  $y(t)$ . In this paper,  $A$  is obtained by experiments.

In Eq. (1),  $m$  is known value as mass summation of pantograph type link and caterpillar track wheel. But parameters of  $b$  and  $k$  are unknown values. The unknown parameters are estimated by process model identification method [6].

### 3.2 Model identification

To estimate the unknown parameters, input and output of plant without wall-pressing force  $F$  are used. Fig. 6 shows simulated model outputs and measured plant outputs using 3Hz lowpass filter when pulse signal input is given to model.

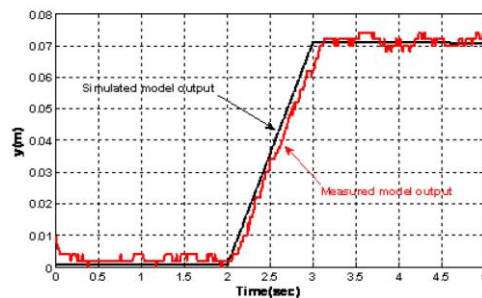


Fig. 6 Measured and simulated model outputs with pulse input  $u = 90N$ .

From Fig. 6, nominal model of pantograph type link without wall-pressing force is derived into Eq. (3) with 91% fitting rate.

$$G_m(s) = \frac{Y(s)}{U(s)} = \frac{1}{7s^2 + 3886.7972s + 1} \quad (3)$$

Fig. 7 shows simulated model outputs and measured plant outputs when step signal input 90N is given to model.

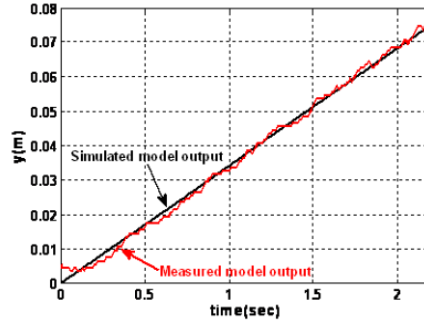


Fig. 7 Measured and simulated model outputs with step input  $u = 90N$ .

The results of identification show that nominal model Eq. (3) is satisfied with plant of pantograph type link from Fig. 7.

#### IV. DESIGN OF THE WALL-PRESSING FORCE OBSERVER

The wall-pressing force of the wall-press type robot must always be constant to drive in pipeline such as horizontal and vertical pipeline. If the wall-pressing force is not constant, the robot gets jammed in pipeline. This problem occurs due to failures to maintain a steady position and driving. Thus, an appropriated wall-pressing force is required to the inpipe inspection robot. The previous wall-press type inpipe inspection robot generated the wall-pressing force using spring tensions [1]. Therefore, because of the limitation of a spring constant, this method cannot keep constant wall-pressing force in large variable pipe diameter. A method of generating the wall-pressing force by DC motor is proposed. But it is difficult to know the wall-pressing force in pipeline exactly without using a force sensor. Moreover, the more sensors are used, the more defects appear to inpipe inspection robot when the inpipe inspection robot drives in the field. An observer is needed to estimate the unknown wall-pressing force. The wall-pressing force observer is designed by nominal model of Eq. (3) as shown in Fig. 8.

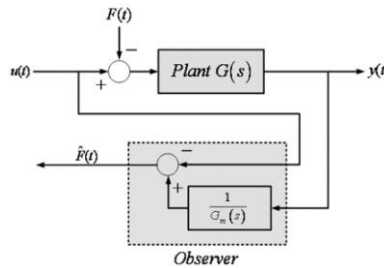
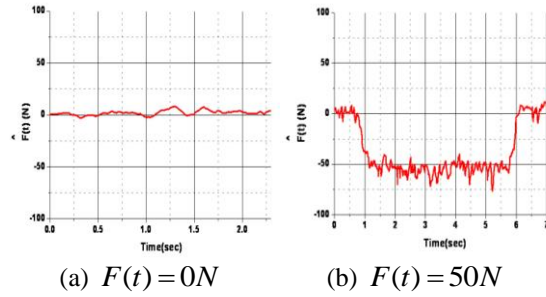


Fig. 8 Block diagram of the wall-pressing force.

The designed wall-pressing force observer equation is given as follows:

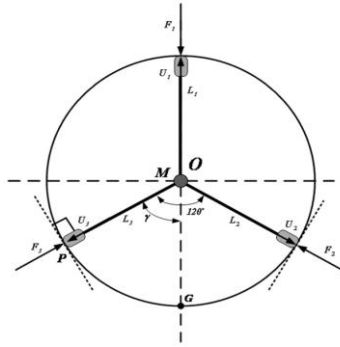
$$\hat{F}(s) = \frac{Y(s)}{G_m(s)} - U(s) \quad (4)$$

The effectiveness of the designed wall-pressing force observer is shown from the experimental results in Fig. 9. Fig. 9 is outputs of the wall-pressing force observer when  $F(t) = 0N$  and  $F(t) = 50N$ , respectively. Fig. 9 (a) shows that the estimated wall-pressing force is about 0N. Fig. 9 (b) shows that the estimated force is about 50N. The experimental results show that the designed wall-pressing force observer is effective to estimate the unknown wall-pressing force.


 Fig. 9 Experiment of observer in  $u(t) = 80N$ 

### V. ALGORITHM FOR THE WALL-PRESSING FORCE GENERATION

To find out the appropriate wall-pressing force for the inpipe inspection robot to be sustained in pipeline, the following algorithm is discussed. As shown in Fig. 10, when the center position of the inpipe inspection robot is equal to the center of the pipeline and  $\gamma = 60^\circ$ , the wall-pressing force of pantograph type links of  $L_2$  and  $L_3$  is derived as Eq. (5) [3].


 Fig. 10. Model of inpipe inspection robot in  $\gamma = 60^\circ$ .

$$F_2 = F_3 = \frac{1}{2}Mg \quad (5)$$

To improve the driving performance of the inpipe inspection robot in pipeline, wall-pressing forces of each pantograph type link are similar to those of the mobile robot on the ground. If  $U_1$  is  $Mg$ , all of wall-pressing forces are same with Eq. (6). In this paper, Eq. (6) is defined as a reference value of the wall-pressing force.

$$F_1 = F_2 = F_3 = Mg \quad (6)$$

### VI. DESIGN OF THE WALL-PRESSING FORCE CONTROLLER

To track the reference value  $F_i$  of the wall-pressing force, a PID fuzzy controller is designed. The controller is designed so that the error  $e(t)$  between the estimated wall-pressing force  $\hat{F}(t)$  and the reference value of the wall-pressing force  $F_i$  goes to zero. The wall-pressing force PID fuzzy controller is depicted in Fig. 11.

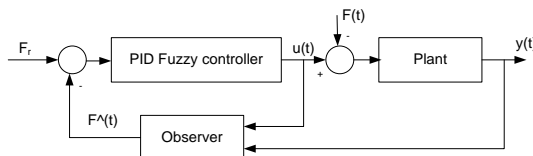


Fig. 11. Block diagram of PID Fuzzy controller.

### VII. EXPERIMENTAL RESULTS

To verify the PID fuzzy controller, the experimental results are shown in Fig. 12~15 when the reference wall-pressing force  $F_i$  is  $50N$ . The conditions of experiments are listed in Table 3.

Table 3 Conditions of experiments.

| Time (sec)    | Wall-pressing force $F(t)$ (N) |
|---------------|--------------------------------|
| About 0~0.5   | 0                              |
| About 0.5~3.5 | 50                             |
| About 3.5~4.5 | 100                            |
| About 4.5~5.5 | 50                             |
| About 5.5~7.0 | 0                              |
| About 7.0~8.0 | 50                             |

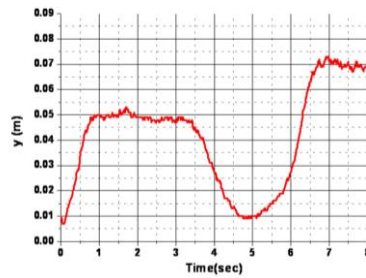


Fig. 12. Displacement of pantograph.

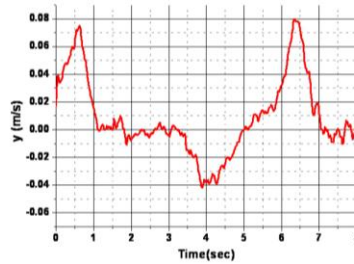


Fig. 13. Velocity of pantograph link.

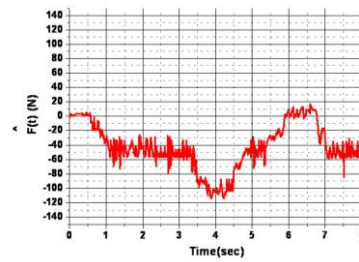


Fig. 14. Observer output.

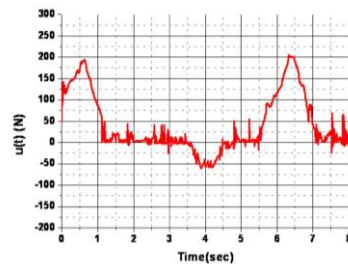


Fig. 15. Control input.



In Figs. 12~15, when the estimated wall-pressing force is larger than the reference wall-pressing force, the displacement of the pantograph type link is decreased in the  $y$  direction. The control input and the velocity of pantograph type link are decreased to minus value. When the estimated wall-pressing force is smaller than the reference wall-pressing force, the displacement of the pantograph type link is increased in the  $y$  direction. The control input and the velocity of pantograph type link are increased to plus value. When the estimated wall-pressing force is equal to the reference wall-pressing force, the pantograph type link is stopped. The control input and the velocity of pantograph type link go to zero. The wall-pressing force observer estimates the wall-pressing force well for all conditions of experiments. The inpipe inspection robot is tested in pipeline with applying the wall-pressing force PID fuzzy controller to three pantograph type links spaced in  $120^\circ$ . Figs. 16~17 show results of driving tests in the horizontal straight and  $30^\circ$  slope straight pipelines with the diameter of 0.8m, respectively.

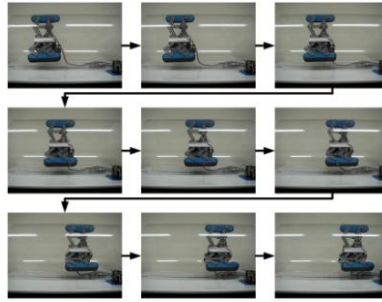


Fig. 16. Driving tests in the straight pipeline.

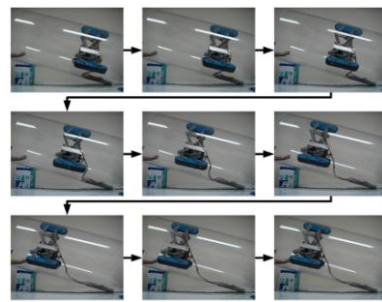


Fig. 17. Driving tests in  $30^\circ$  slope pipeline.

Fig. 18 shows test results of wall-pressing force PID fuzzy controller in each pantograph type link.

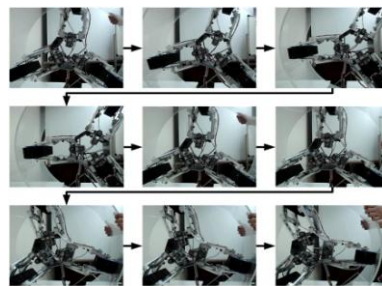


Fig. 18. Test of wall-pressing force in each pantograph type link.

The inpipe inspection robot drives in the straight pipeline and slope pipeline smoothly. The PID fuzzy controller in each pantograph type link is efficient to control the wall-pressing force.

### VIII. CONCLUSION

This paper presents development results of an inpipe inspection robot. Its mechanical design is designed by 3D machine design program. The control module consists of a micro controller, motor driver and sensor interface. To control the inpipe inspection robot, firstly, when the inpipe inspection robot was considered as a mass-spring-damper system, the dynamic model of the system was obtained by process model identification method. Secondly, an observer was designed to estimate the unknown wall-pressing force to sustain the inpipe inspection robot in pipeline. Thirdly, an algorithm of wall-pressing force generator was



presented to find out an appropriate wall-pressing force, and the appropriate wall-pressing force was given as a reference value of wall-pressing force. Fourthly, PID fuzzy controller was designed to make the estimated wall-pressing force track the reference wall-pressing force irrelatively to variable diameter of pipeline. Finally, the driving tests of the inpipe inspection robot were performed in horizontal pipelines and slope pipelines of 30°. The test results were shown to prove the effectiveness of the developed inpipe inspection robot.

#### REFERENCES

- [1] S. G. Roh and H. Choi, Strategy for navigation inside pipelines with differential-drive inpipe robot, IEEE International Conference on Robotics and Automation 2002, Vol. 3(2002), pp. 2575-2580.
- [2] A. A. F. Nassiraei, Y. Kawanura, A. Ahrary, Y. Mikuriya and K. Ishii, Concept and design of a fully autonomous sewer pipe inspection mobile robot 'KANTARO', IEEE International Conference on Robotics and Automation(2007), pp. 136-143.
- [3] Y. Zhang and G. Yan, In-pipe inspection robot with active pipe-diameter adaptability and automatic tractive force adjusting, Mechanism and Machine Theory, Vol. 42, No. 12(2007), pp. 1618-1631.
- [4] H. T. Roman, B. A. Pellegrino and W. R. Sigrist, Pipe Crawling Inspection Robots, IEEE Trans. Energy Convers., Vol. 8(1993), pp. 576-583.
- [5] A. M. Bertetto and M. Ruggiu, In-pipe Inch -Worm Pneumatic Flexible Robot, Proc. IEEE/ASME Int. Conf. Advanced Intelligent Mechatronics, Vol. 2(2001), pp. 1226-1231.
- [6] S. C. Chung and M. S. Kim, Integrated design of servomechanisms using a disturbance observer, Trans. of KSME (A), Vol. 29, No. 4(2005), pp. 591-599.